

Study of the Influence of Coating Roughness on the Properties and Wear Resistance of Electrosark Deposited Ti6Al4V Titanium Alloy

Todor Penyashki^{a,*}, Georgi Kostadinov^a, Mara Kandeveva^b, Antonio Nikolov^b, Rayna Dimitrova^b, Valentin Kamburov^b, Pancho Danailov^b, Snezhan Bozhkov^a

^aInstitute of Soil Science, Agrotechnologies and Plant Protection „N. Pushkarov“, Agricultural Academy, Sofia, Bulgaria,

^bTechnical University of Sofia, Bulgaria.

Keywords:

Electrosark deposition
Coatings
Surface roughness
Microhardness
Wear resistance

* Corresponding author:

Todor Penyashki 
E-mail: tpeniashki@abv.bg

Received: 30 June 2023

Revised: 28 July 2023

Accepted: 15 August 2023



ABSTRACT

The present work is concerned with studying surface parameters of coatings deposited to titanium alloy Ti6Al4V by electrosark deposition (ESD) with hard alloy depositing electrodes based on WC, TiC and TiCN. The variation of roughness parameters, composition, structure and tribological characteristics of coatings as a function of ESD mode parameters was investigated. The influence of the mode parameters on the main coating roughness parameters (R_a , R_z , R_{max} , R_{pk} , R_k , R_s , R_{sk} , R_{ku} (ISO 21920-2:2021) was analysed, the values of which can be used to determine the load bearing capacity and wear resistance. The results of the tribological tests showed that within the test range, the roughness of the coatings has a controversial influence on their frictional wear performance. As the roughness parameters increase to $R_a=3\div3.5\ \mu\text{m}$, the relative wear resistance of the coated surfaces also increases, reaching values up to $4\div5\ \mu\text{m}$ for the electrodes used and no significant changes in the wear mechanism were observed. However, increasing coating roughness above $R_a=3.5$ to $5\ \mu\text{m}$ results in a monotonic decrease in relative wear resistance to $2.5\div3$ times. Possible ways to reduce the surface roughness and increase the wear resistance of coatings were presented.

© 2024 Published by Faculty of Engineering

1. INTRODUCTION

Various surface modification methods such as ion plasma nitriding [1,2], chemical and physical vapor deposition CVD and PVD [3,4], gas flame spraying [5,6], etc., are currently used to improve the low hardness, relatively high coefficient of friction, tendency to adhesive

bonding and intense wear and failure of the titanium and its alloys [1-8]. Complex, energy-intensive, expensive installations and complicated technologies, high process time, annealing, recrystallization and thermal deformation of the substrate caused by high temperatures, inability to deposit more thickness coatings and insufficient adhesion,

high costs and environmental pollution are some of the main difficulties limiting the use of these methods.

A suitable method to solve these predicaments is the Electrospark Deposition (ESD). Without special surface preparation, volume heating, by selecting appropriate electrode materials and mode parameters by ESD on the titanium surfaces, hard, wear-resistant coatings with anticorrosion, and other functional properties can be obtained [9-11]. ESD processing can provide significant advantages over the methods mentioned above, such as high bond strength to the substrate material, insignificant heating and absence of deformation of the coated product, simple, universal and inexpensive technology and equipment, easy operation, low material consumption, low energy and work intensity and high environmental friendliness [9,12-15].

A main disadvantage of ESD coatings on titanium surfaces is their relatively high roughness, which reduces the effect of their application. It is known [16-18] that surface roughness and texture play an important role on the coefficient of friction values and the wear characteristics. In tribology, rough surfaces typically have higher coefficients of friction and wear out more quickly [18-21].

The analysis of literature data shows that the most important process parameters in terms of the roughness of the coatings are the pulse energy, the type of electrode material and the initial roughness of the substrate. The influence of texture and roughness on the wear resistance of ESD coatings is too complicated to be study because the change in roughness is always accompanied by a change in the thickness, phase composition and structure of the coatings. It is widely known [10-12,14-16,22] that as the pulse energy increases, the amount of electrode material transferred to the substrate increases. The roughness, the thickness, microhardness, and the amount of wear-resistant phases in the formed layer increase accordingly. The combining of low roughness with high coating density and hardness, and higher electrode material transfer are controversial objectives that require the study of the relations between process parameters, roughness, thickness and structure of coatings and their wear resistance.

In this regard, the aim of the present work is to study the influence of the energy parameters of the ESD process on the roughness and tribological behavior of the coated surfaces and justifying the prerequisites for creating a hard and wear-resistant layer with reduced roughness on titanium and titanium alloy Ti6Al4V.

2. MATERIALS AND METHODS

2.1 ECD equipment, substrates, electrodes

ECD equipment: Two types of low pulse energy equipment were used:

- Manual device with vibrating electrode - "Carbide Hardedge" (England, USA) with the following parameters: short circuit current - $0.2 \div 1.5$ A, voltage- U - 80 V, oscillation frequency of the vibrator 200 Hz, and modes with parameters given in Table 1. Coatings were applied with three and five electrode passes at $\approx 0.6 \div 1$ mm/s;
- Apparatus for non-contact local electrospark deposition (LESDD) - US Patents /3832514 and US /4226697, - at which coatings were applied by a cylindrical rotating electrode. During the coating deposition, the workpiece was moved at a controlled speed along two axes, and an automatic regulator maintains the required inter-electrode distance for the plasma spark discharges take place. Modes with the following parameters were used: pulse current amplitude $I=12.8 \div 24.4$ A; capacitance $C=0.68 \div 4.4$ μ F; pulse duration $T_i=8 \div 20$ μ s; pulse frequency $f=5 \div 12.5$ kHz; coating speed $0.5 \div 1.0$ mm/s; number of electrode passes - $n=2 \div 4$, electrode rotation speed 800 rpm and pulse energy $E=0.005 \div 0.045$ J.

Table 1. Regimes for ESD whit vibrating electrode.

Nº of regimes	1	2	3	4	5	6
Capacity, μ F	1.5	3.5	5	7	10	20
Pulse energy $E \cdot 10^{-2}, J$	0.5	1	1.6	2	3	7

Substrates: Model plates with different initial roughness of titanium alloy Ti6Al4V (Gr5) and of technical titanium Ti-GR2 (AISI UNS R R56200 and R50400) produced by 3D printing and by electrical discharge machining (EDM) were used.

Electrodes: Hard-alloy and metal electrodes with the composition and designations shown in Table 2 were used.

Table 2. Chemical composition of ESD electrodes.

Type of electrode	Chemical composition
NWW10T10B10 (NW)	50%WC+10%TiB ₂ +10% B ₄ C+(Ni-Cr-B-Si-C)-bal.
KW10T10B10 (KW)	55%WC+20%TiB ₂ +10% B ₄ C+(Ni-Cr-B-Si-C)-bal.
TN	TiN+14%(Ni+Cr)+1-2% (Cu-B-Al ₂ O ₃ -C)
KNT16	TiCN+19.5%Ni+6.5%Mo)
TiB ₂ -TiAl _{nano}	93%(74%Ti+12%TiB ₂ +14%Al) + 7% _{nano} (NbC+ZrO ₂) [13]
AlSi9	9%Si +Al
AlSi12	12%Si +Al

2.2 Methodology of measurements, research equipment

The roughness of the coatings was measured with profilometers - "Surtronic 3+", "TESA Rugosurf 10-10G" and "AR-132B" according to ENISO13565-2:1998), DIN 4776, ISO 4287:1997, ENISO4287 and ISO25178 standards. The specimens were measured in three sections in two mutually perpendicular directions for each section. After determining the standard deviation and the confidence interval, the results are the average of 5 parallel measurements.

The thickness δ of the coatings was determined with an indicator clock with an accuracy of 0.001 mm. Taking into account the friction processes and the conditions of contact plastic and elastic deformations and stress concentration, and also the data presented in [17-21] on the correlation of the roughness parameters with the coefficient of friction, the following parameters were selected for evaluation the roughness of the deposited coatings:

- R_a , μm - average roughness – the generally accepted integral parameter - most used for describing surfaces;
- R_q , μm - root mean square roughness taking into account the average-geometric value of the profile deviations from the midline, which corresponds to the R_a parameter;
- R_{max} and R_t - most researchers affirm that these are the most significant parameters affecting friction [17,24,25]. R_t is the maximum roughness height ($R_t=R_p + R_v$,

defined by the maximum height R_p of the protrusions and depth R_v of the troughs), and R_{max} , is the maximum roughness depth;

- R_z , μm - average of the 5 highest protrusions and 5 deepest troughs of the profile within the baseline length;
- R_{pm} , μm - average maximum profile peak height – the average of the obtained maximum values of protrusions (peaks) R_{pi} for each base length;
- R_{sk} , the distribution asymmetry (Skewness) parameter, is a measure of the degree of symmetry of the amplitudes distribution curve of the profile roughness around the midline;
- R_{ku} - the excess (sharpness) distribution parameter (Kurtosis) is a measure of the shape of the distribution curve of the profile amplitudes.
- R_k - core roughness depth - from the Abbott curve for the reference profile length;
- R_{pk} - reduced peak height – height of the material at the peak of the ridges;
- R_s - the average of the distances between two adjacent peaks;
- R_{sm} - the average distance between the peaks of the profile along the midline;
- waviness W_t - maximum depth of waviness (primary roughness) of the irregularity profile.

A Zwick 4350 hardness tester at a load of 2 N was used to study the coating microhardness (HV) according to ISO 6506-1:2014.

The microstructural analysis, topography analysis and morphology analysis of the coatings were carried out with an optical and scanning electron microscope (SEM-EDS) "EVO MA 10 Carl Zeiss" with built-in X-ray microanalyzer EDX system "Bruker".

The "CSM REVETEST Scratch Macrotester" was used to compare and digitally record the coefficient of friction (μ) and tangential force (F_t) of coatings under increasing normal load from 0 to 50 N at a rate of 10 N/mm.

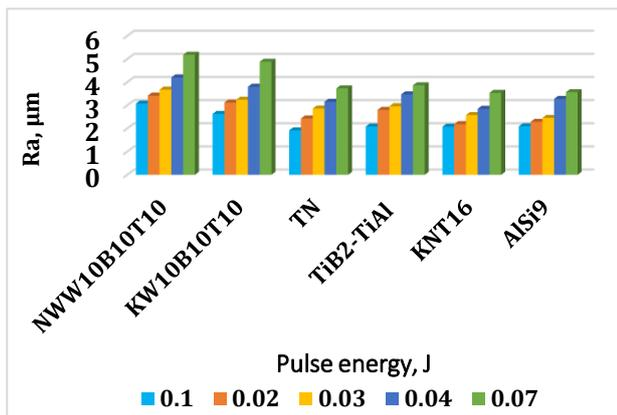
Abrasive wear of coated surfaces was studied by comparative tests with a "thumb-on-disc" type tribotester in dry friction with fixed abrasive particles in planar contact under the following

conditions: normal load 5 N; nominal contact pressure 1.74 N/cm²; disc rotation speed 60 rpm; sliding speed 0.239 m/s; abrasive surface - Corundum №1200. Mass wear was defined as the difference between the initial mass of the specimen "m₀" and its mass "m_i" after a certain number of friction cycles: $m = m_0 - m_i$, mg. The wear intensity was defined as the amount of wear per unit friction work: $I = m / (P.L)$, mg/Nm, where m is the solid wear for the test time, P the normal load, L the friction path travelled. Wear resistance is defined as the reciprocal of wear intensity.

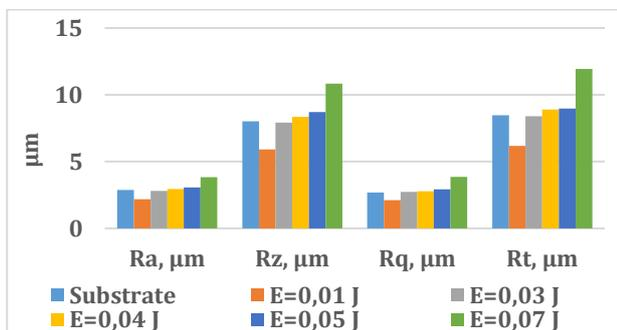
3. RESULTS AND DISCUSSION

3.1 Roughness, thickness, structure and micro-hardness of coatings

Fig. 1 shows the average roughness R_a of coatings on Ti6Al4V with an initial roughness R_a ≈ 2,5 μm as a function of pulse energy at ESD with a vibrating electrode.



(a) Roughness Ra of coatings, substrate R_a ≈ 2.5 μm



(b) electrode AlSi12 substrate R_a ≈ 2.5 μm

Fig. 1. Roughness of coatings on Ti6Al4V vs. the pulse energy.

Fig. 2. shows the average roughness R_a and her coefficient of variation at the coatings of electrode AlSi12 on Ti6Al4V as a function of the pulse energy at the ESD.

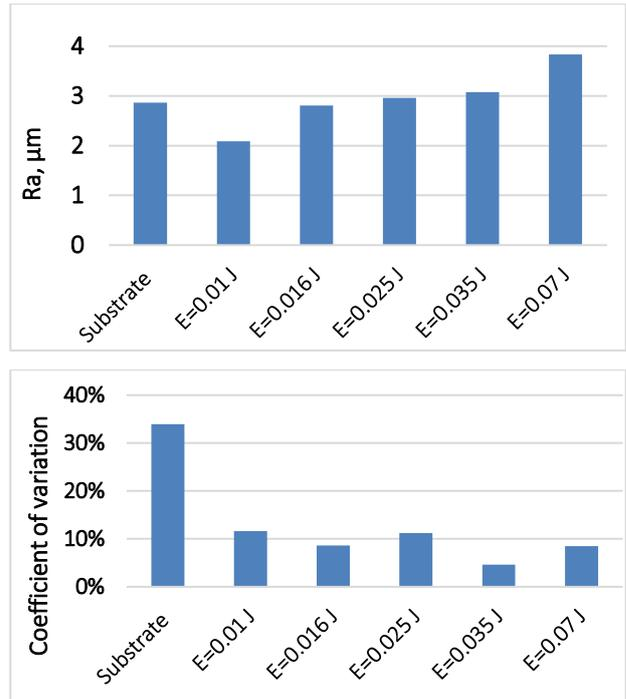


Fig. 2. Average roughness R_a, and coefficient of variation/vs the pulse energy of AlSi12 ESD coatings on Ti6Al4V at initial roughness R_a ≈ 3 μm [22].

Table 3 presents the roughness height parameters, the thickness δ and microhardness HV of LESD coatings deposited on Ti6Al4V substrate, produced by 3D printing and SLM. The coatings were deposited with two and three consecutive passes of the electrode at pulse energies E = 0.02 J and E=0.04 J.

Table 3. Roughness, thickness δ and microhardness HV of coatings on SLM Ti6Al4V substrates [22].

Nº	Parameter/Type of the electrode	R _a , μm	R _z , μm	R _q , μm
0	substrate Ti6Al4V	8.92	23.38	8.83
1	NW, E=0.02 J, 3 pass	3.47	9.8	3.29
2	NW, E=0.04 J, 3 pass	4.81	13.59	4.91
5	KW, E=0.02 J, 2 pass	3.4	9.55	3.36
6	KW, E=0.04 J, 2 pass	4.33	13.12	4.49
7	AlSi9, E=0.02, 2 pass	2.29	6.47	2.3
7	AlSi9, E=0.03, 2 pass	2.46	6.9	2.48
8	AlSi9, E=0.04, 2 pass	3.28	11.17	4.02
9	AlSi9, E=0.04, 3 pass	3.37	11.77	4.37
Nº	Parameter/Type of the electrode	R _t , μm	δ, μm	HV, GPa
0	substrate Ti6Al4V	24.6	-	3.75
1	NW, E=0.02 J, 3 pass	10.48	10.75	9.85
2	NW, E=0.04 J, 3 pass	14.22	18.53	12.34
5	KW, E=0.02 J, 2 pass	10.74	9.67	11.87
6	KW, E=0.04 J, 2 pass	16.63	14.66	12.22
7	AlSi9, E=0.02 J, 2 pass	6.54	6.7	8.03
7	AlSi9, E=0.03 J, 2 pass	6.97	8.6	7.86
8	AlSi9, E=0.04 J, 2 pass	11.38	9.55	9.43
9	AlSi9, E=0.04 J, 3 pass	12.1	11.11	9.67

Fig. 3 shows the height roughness parameters of LESD coatings deposited with different pulse energy on 3D titanium substrate.

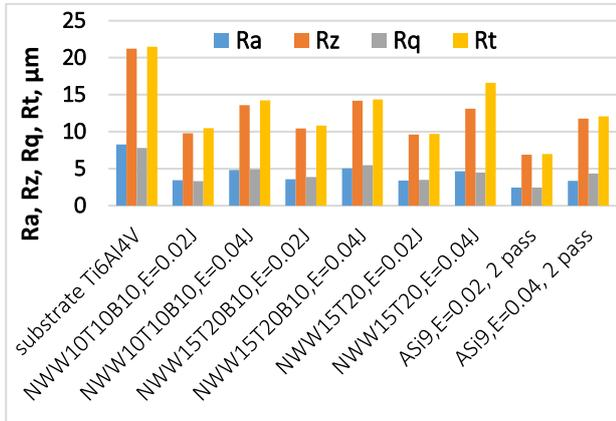


Fig. 3. Height roughness parameters of LESD coatings deposited on SLM substrate.

Table 4 [12] shows the values of R_a parameter, thickness and microhardness of ESD coatings deposited on Ti6Al4V substrate with initial roughness $R_a=1.7 \mu\text{m}$.

Table 5 presents the height, step and functional roughness parameters of ESD coatings deposited on Ti6Al4V with initial roughness $R_a \approx 0.2 \mu\text{m}$. Fig. 4 compares the coating roughness parameters of the studied electrodes at different pulse energy.

Comparing the characteristics of the coatings shows (Tables 3 and 4) that the hardness of all deposited coatings exceeds up to 2-3 times the hardness of the base metal Ti6Al4V.

Table 5. Surface parameters of ESD coatings at initial roughness of the base $R_a = 0.2 \mu\text{m}$.

Parameter	TN 0.03J	TN 0.07J	AlSi12 0.07J	KNT16 0.03J	KNT16 0.07J	KW 0.03J	KW 0.07J	NW 0.07J	TiB ₂ -TiAl 0.03J	TiB ₂ -TiAl 0.07J	Ti6Al4V
$R_a, \mu\text{m}$	2.22	2.52	3.16	2.16	2.35	3.26	4.53	5.1	2.2	3.26	0.304
$R_q, \mu\text{m}$	2.92	3.23	4.02	2.77	2.93	4.12	6.02	6.33	2.8	4.15	0.53
$R_t, \mu\text{m}$	19.4	22.3	25.62	17.02	22.25	26.2	35.8	35.9	17.4	28.3	4.46
$R_z, \mu\text{m}$	13.7	14.3	18.4	13.04	13.15	17.7	27.7	29.2	13.5	17.8	1.88
$R_{pm}, \mu\text{m}$	6.67	6.83	7.06	5.77	6.7	8.33	14.6	14.5	5.61	6.94	0.94
R_{sk}	-0.17	-0.23	-0.65	-0.21	-0.26	-0.12	0.09	0.11	-0.84	-0.68	-1.05
R_{ku}	3.19	3.35	3.35	3.67	3.56	3.23	4.31	2.93	3.75	4.25	6.68
$R_y, \mu\text{m}$	18.0	17.9	22.7	17.2	20.5	22.6	33.9	33.3	17.23	26.81	4.55
$R_{kz}, \mu\text{m}$	8.22	8,15	10.51	6,86	7.46	9.27	13.6	14.7	6.91	9.19	0.545
$R_{pk}, \mu\text{m}$	8.4	4.83	5.841	7.01	8.18	5.24	5.84	9.63	3.33	5.15	2.85
W_t	7.4	8.31	11.72	7.38	9.53	11.	15.2	17.3	10.42	16.83	3.13
R_s	34.4	41.7	43.2	35.54	42.6	44.1	55.0	47.0	56.0	36.0	33.0
R_{sm}	88.4	104	104.8	85.72	111	107	118	126	164.3	136.7	68
R_s	2.2	5.8	4.7	4.2	6	5.8	4.2	3.1	13.6	5.7	9.6

Table 4. Roughness R_a , thickness δ and microhardness HV of ESD coatings on titanium alloy Ti6Al4V at initial roughness of the base $R_a=1.67 \mu\text{m}$ -[12].

Parameter /Electrode	E, J	$R_a, \mu\text{m}$	$\delta, \mu\text{m}$	HV, GPa
TN	0.03	2,3	11	9.85
TN	0.07	2,86	14	10.3
KNT16	0.03	2.16	16	11.2
KNT16	0.07	2.34	16	12.4
TiB ₂ -TiAl	0.03	2.8	11	12.4
TiB ₂ -TiAl	0.07	3.41	15	11.8
KW10B10T10	0.03	3.25	14	11.5
KW10B10T10	0.07	4.16	18	11,6
NWW10B10T10	0.03	3.49	17	11.6
NWW10B10T10	0.07	5.45	25	12.3
AlSi12	0.03	2.68	12	8.6
AlSi12	0.07	3.19	15	8.9
Ti6Al4V (base)	-	1.67	-	3.71

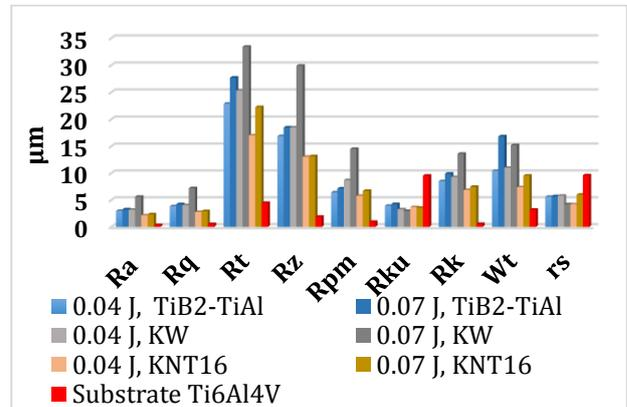


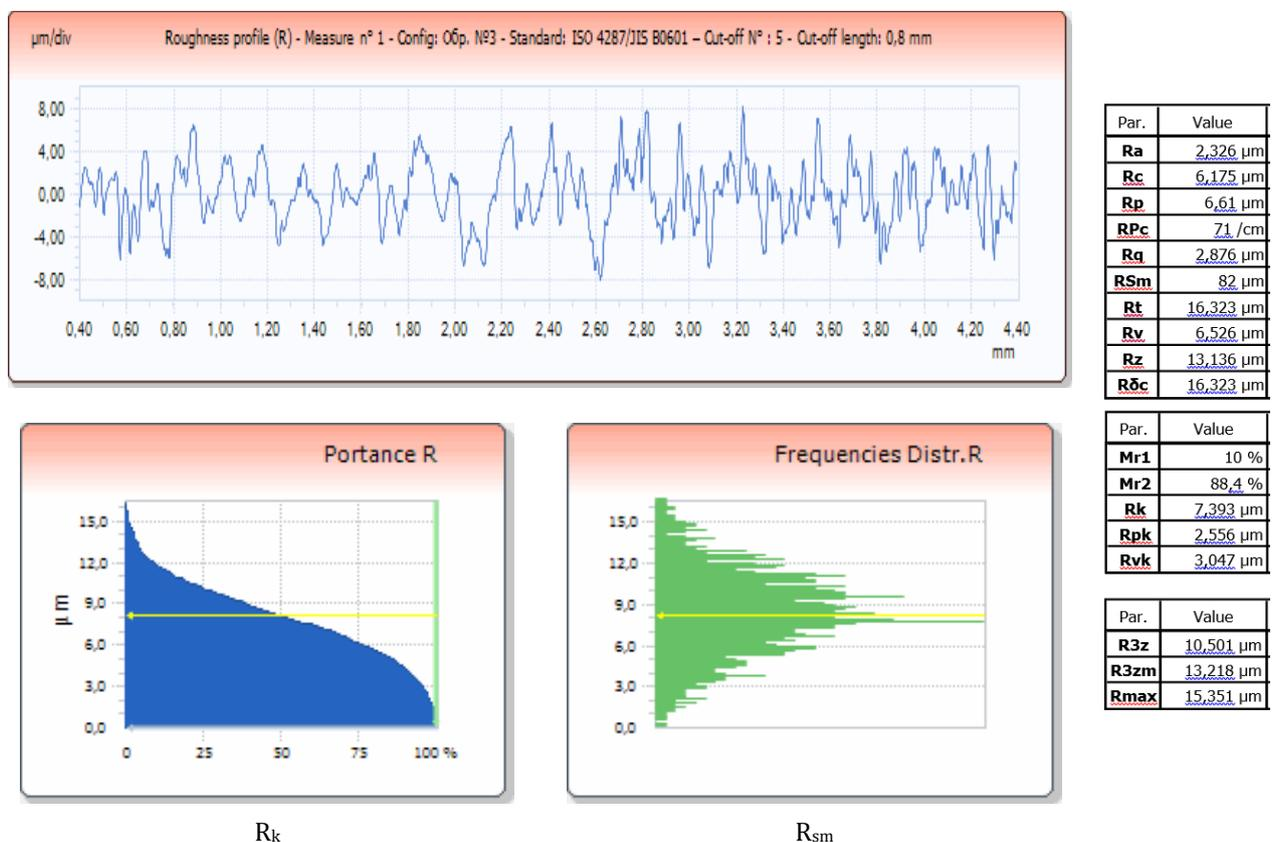
Fig. 4. Roughness parameters of coatings on Ti6Al4V as a function of the energy of the pulses at initial roughness of the base $R_a = 0.3 \mu\text{m}$.

Table 6. Roughness R_a and thickness δ of coatings with AlSi12 electrodes on different substrates with different initial roughness.

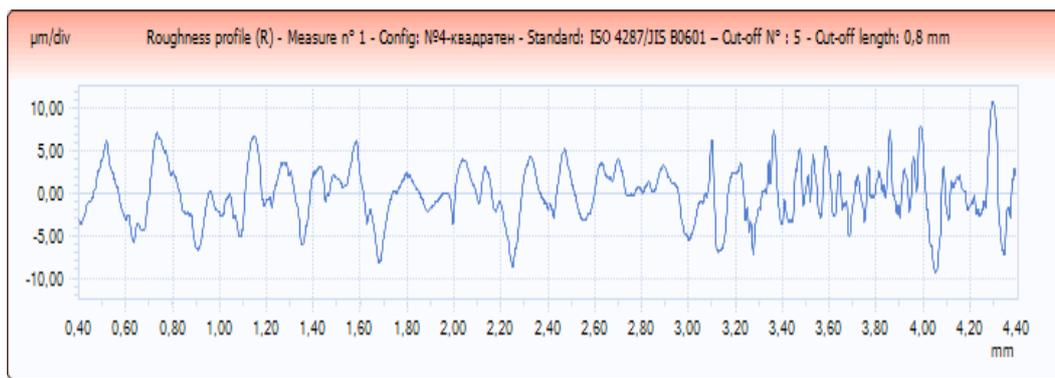
Substrate	Process parameters	$R_a, \mu\text{m}$	$R_z, \mu\text{m}$	$R_q, \mu\text{m}$	$R_t, \mu\text{m}$	$\delta, \mu\text{m}$
GR2	Uncoated	2.9	8.5	3.48	8.9	-
GR2	ESD- E=0.03 J	4.27	12.1	4.23	12.9	10
GR2	ESD- E=0.07 J	4.92	14.18	4.85	14.8	15
GR2	LESD-E=0.015 J	1.22	3.45	1.32	3.5	6
GR2	LESD-E=0.02 J	1.29	3.64	1.3	3.6	8
GR2	LESD-E=0.03 J	1.7	4.1	1.8	-	9
GR2	LESD- E=0.045 J	2.9	8.2	2.9	8.6	14
GR5	Uncoated	4.32	12.6	4.47	13.5	-
GR5	LESD-E=0.02 J	1.7	4.8	1.92	4.66	7
GR5	LESD-E=0.045 J	2.87	8.02	2.68	8.46	11
GR5	ESD- E=0.02 J	3.08	8.70	3.12	8.80	9
GR5	ESD- E=0.03 J	3.56	10.1	3.6	10.2	11
GR5	ESD- E=0.07 J	3.83	10.8	3.87	10.9	16

Table 6 shows the roughness parameters of some of the coatings obtained by vibrating electrode ESD and by LESD on substrates with different initial roughness, depending on the pulse energy.

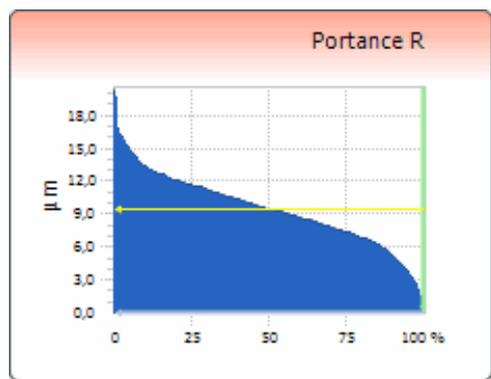
Fig. 5 shows the surface profilograms and measured surface roughness parameters of ESD coatings deposited with KW electrodes on Ti6Al4V substrate deposited at different pulse energies.



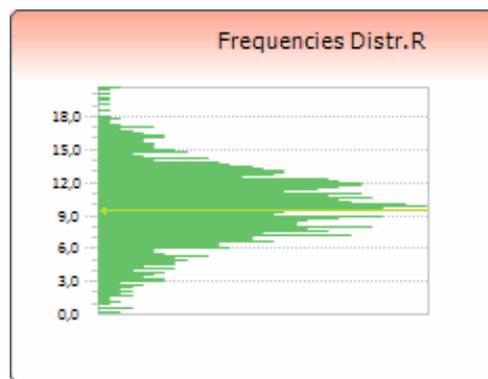
(a) Ti6Al4V obtained by EDM



Par.	Value
Ra	2,548 µm
Rc	7,261 µm
Rp	5,9 µm
RPc	33 / cm
Rq	3,082 µm
RSm	224 µm
Rt	17,426 µm
Rv	6,381 µm
Rz	12,281 µm
Rδc	17,426 µm



R_k

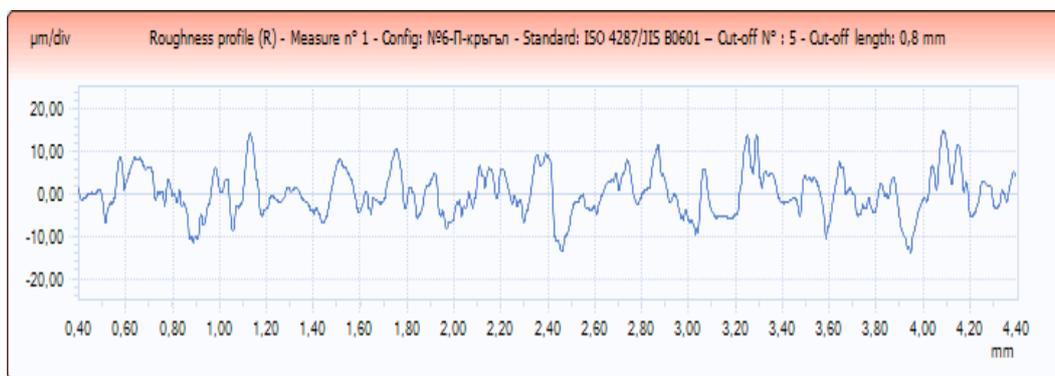


R_{sm}

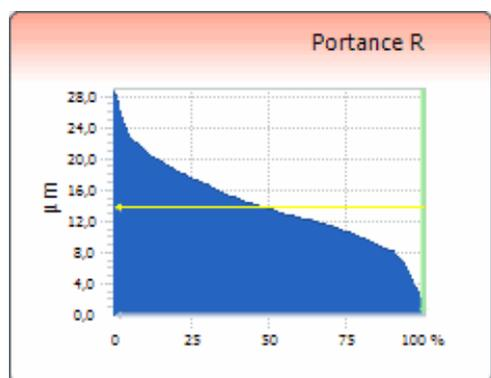
Par.	Value
Mr1	6,4 %
Mr2	90 %
Rk	9,118 µm
Rpk	3,336 µm
Rvk	2,952 µm

Par.	Value
R3z	5,793 µm
R3zm	7,01 µm
Rmax	15,702 µm

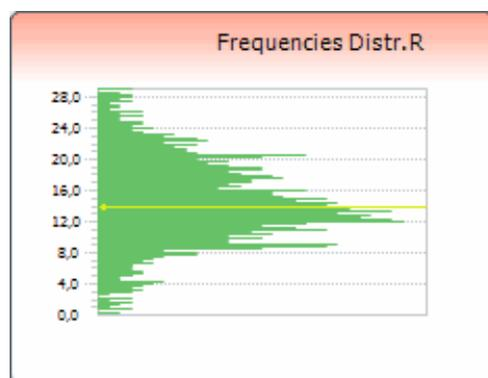
(b) ESD coating by electrode KW10J10B10 on Ti6Al4V, E=0.03 J



Par.	Value
Ra	4,095 µm
Rc	11,326 µm
Rp	12,63 µm
RPc	51 / cm
Rq	5,167 µm
RSm	140 µm
Rt	28,696 µm
Rv	11,515 µm
Rz	24,145 µm
Rδc	28,696 µm



R_k



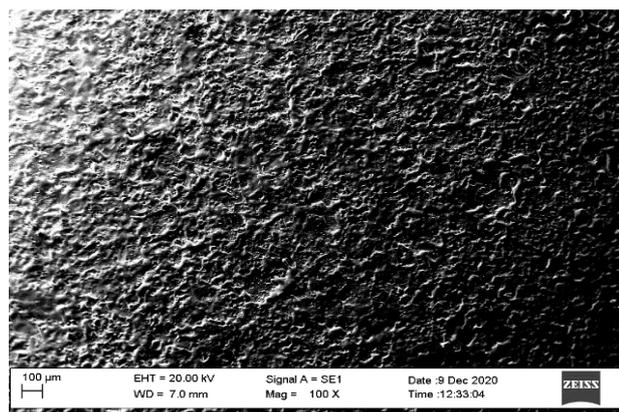
R_{sm}

Par.	Value
Mr1	14,5 %
Mr2	90,7 %
Rk	12,381 µm
Rpk	5,653 µm
Rvk	6,217 µm

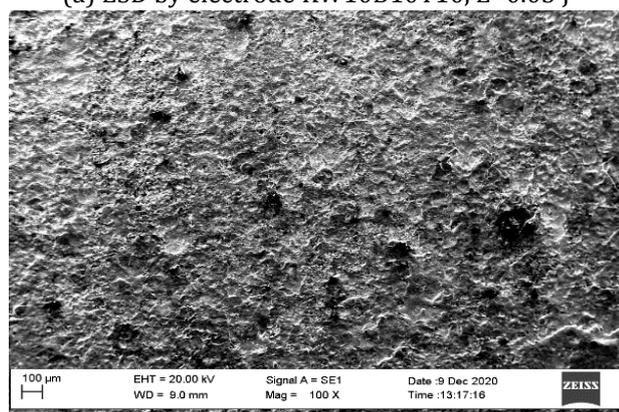
Par.	Value
R3z	14,095 µm
R3zm	17,774 µm
Rmax	28,696 µm

(c) LESD coating by electrode KW10J10B10 on Ti6Al4V, E=0.04 J [12]

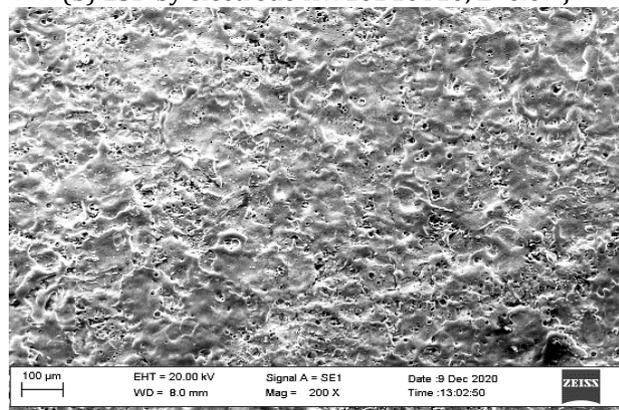
Fig. 5. Profilograms and surface roughness parameters of ESD electrode coatings KW10B10T10 on Ti6Al4V substrate.



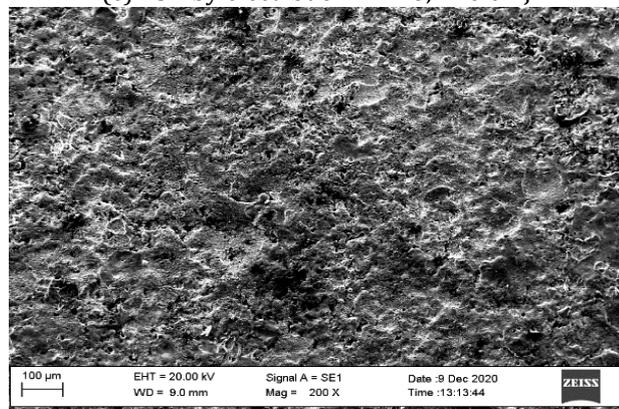
(a) ESD by electrode KW10B10T10, E=0.03 J



(b) ESD by electrode KW10B10T10, E=0.07 J



(c) ESD by electrode KNT 16, E=0.04 J



(d) ESD by electrode KNT 16, E=0.07 J [16]

Fig. 6. SEM topography of ESD coatings on TiAl6V4 with KW10B10T10 and KNT16 electrodes

Figure 6 shows SEM images of the topography of coatings deposited by vibrational ESD with KW and KNT16 electrodes on Ti6Al4V alloy at different magnification. It can be seen from the SEM images presented in Fig. 6 that increasing the pulse energy above $E = 0.05$ J results in a decrease in the quality of the coatings.

At these energies, more intense heating of the electrodes occurs, contributing to brittle fracture of the electrode, predominant solid-phase erosion, and the appearance of protrusions. The most uniform surface finish was obtained with tungsten-free and nanocomposite electrodes at energies up to 0.04 J.

The surface of the coatings of the multi-component electrodes (Fig. 6, a, b) is more irregular, with a greater number of protrusions and troughs. In this structure, the electroerosional craters and the smooth surface areas between them are distinguished. At higher magnifications, individual microcracks and micro-roughness's are observed on the surface of the coatings. SEM observations show that the surface of the coatings obtained at $E \leq 0.03$ J is the smoothest.

From the data presented here (Tables 3-6 and Fig. 1-6) and from our previous studies, the following syntheses can be drawn:

- As the pulse energy (I, C, Ti) increases the amount of anode material transferred to the cathode increases [10,12,16,22-24], and the thickness, roughness and microhardness of the coatings monotonically increase, but their specific values under the same ESD conditions are different for different electrodes (Tables 3-5, Figs. 1-4). This is a general trend for the roughness and thickness of coatings reported by almost all authors in the literature. By increasing the pulse duration and the energy of the current spark, a wider and deeper crater is formed on the processed surface, which creates higher roughness and more irregularities.
- The amount of solid phases carried by the electrode, the newly formed compounds and the degree of dispersity and amorphousness also increase [16,22-26]. The coatings of KW and NW electrodes, whose thickness is the highest, and the lowest values - of the coatings of TN, KNT16 and AlSi12 electrodes, show the highest values of the roughness parameters.

- After ESD processing, the coatings from all electrodes used, obtained at pulse energies above 0.03 J, show an increase in almost all roughness parameters relative to the original substrate roughness. The values of the parameters R_t , R_z and of the parameters R_{pm} , R_k and W_t also increase as the highest values are reported again for KW and NW electrodes.
- The roughness and thickness parameters of the coatings obtained by the non-contact LESD method with a pulse duration of up to 20 μs and a high pulse frequency of 1÷12.5 kHz are significantly lower than those obtained by ESD with a vibrating electrode (Table 6, Figs. 1 and 3), and the coatings are more uniform with smaller sized structural components.
- It is found that for surfaces with initial roughness $R_a > 4 \mu\text{m}$ obtained by 3D printing (Fig. 3, Table 3), or after rough and semi-clean processing (Table 6), the LESD and ESD processing with low pulse energy $E \leq 0.03\text{J}$ allows to melt and smooth the roughness from the previous processing, fill the pores and cavities and obtain surfaces with improved uniformity and reduced roughness. Therefore, ESD with these electrodes at pulse energies up to 0.03 J can be used to smooth the micro-roughness of the initial titanium surface, both after 3D printing or after rough mechanical or EDM processing.
- At surfaces with initial roughness $R_a < 3 \mu\text{m}$, after ESD and LESD, most of the coating roughness parameters are higher than those of the initial surface (Figs. 1b,4,5 and Tables 4, 5). However, it is observed that at LESD and ESD of the specimens with initial roughness $R_a \approx 3\text{-}4 \mu\text{m}$, the roughness parameters of the coatings of AlSi12, KNT16 and TN electrodes at pulse energy up to 0.03 J are lower or comparable to those of the original titanium surface (Fig. 1b, Fig. 2, Table 6). As the pulse energy increases up to 0.07 J, the roughness of the coatings increases significantly, and in parallel with R_a , all studied parameters increase except R_s and R_{ku} . It is also notable that the coefficient of variation for the ESD surfaces Fig. 2b is significantly lower than that of the uncoated titanium substrates.
- The skewness (asymmetry) parameter R_{sk} , which is an indicator of the existence of deep troughs or high peaks, in the layered samples (Table 5, Figs. 4 and 5) has a negative value or positive, but close to 0, which predetermines relatively good wear resistance and load bearing properties of the coated surfaces. For the tungsten-free classical electrode specimens, the R_{sk} values are negative and smaller than those for the KW and NW electrodes and generally appear uncorrelated with the pulse energy;
- The parameter R_{ku} (Table 5, Figs. 4 and 5), which determines the sharpness of the shape distribution of the roughness amplitudes, decreases compared to the same parameter at the initial surface - $R_{ku}=6.68$. Melting of the micro protrusions through which the spark discharges flow probably reduces the sharpness of the initial roughness curve and R_{ku} decreases. For most of the specimens, R_{ku} has values close to the optimum $R_{ku} \approx 3$, which is favorable under friction and abrasion conditions because most of the protrusions and troughs are concentrated around the midline of the roughness profile;
- The sum of the roughness parameters $R_{pk} + R_k$, which is mainly related to the contact area, the mechanics of contact and lubricant retention and, according to EN ISO 13565-2: 1998, characterizes the surface wear in the coating area, increases compared to that of the substrate. Higher values of sum can reduce service life and lubrication retention index. The parameter R_k that corresponds to the stable part of the coating surface material is also higher than that of the substrate (Table 5, Figs. 4 and 5). At low pulse energies ($E \leq 0.03\text{J}$), the measured values of R_k for the coatings deposited with the different electrodes are relatively similar, while at pulse energies of 0.07 J the measured values for the NW and KW electrodes are significantly higher. There is also a certain correspondence with the R_a parameter - higher values of R_a correspond to higher values of $R_{pk} + R_k$. When the pulse energy increases above 0.03 J, the sum $R_{pk} + R_k$ also increases, which may characterize the coating surface as less wear resistant in terms of roughness parameters. It can be observed that for the coatings from the tungsten-free electrodes (Table 5, Fig. 4), the

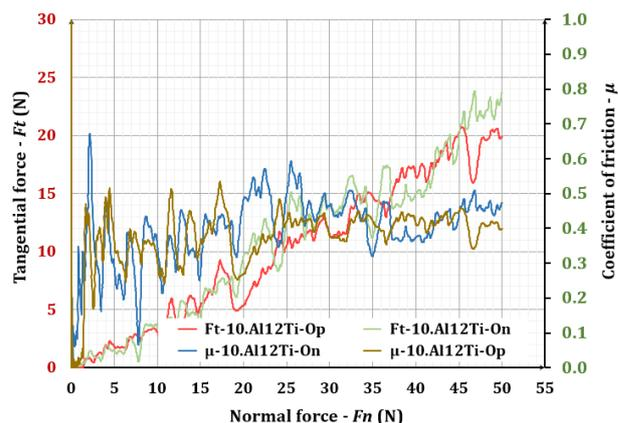
parameter R_{pk} , indicating the material at the peak of the ridges, is smaller compared to the same parameter for the coatings from the KW and NW electrodes;

- The step parameters R_s and R_{sm} , the average distance between the profile peaks along the midline of the coated specimens, are also increased compared to the uncoated surfaces. For the coatings from the tungsten-free electrodes, the parameters have similar values, while for the KW and NW electrodes, the R_s values are larger but uniform. At the lower energy, the values of R_s and R_{sm} are lower than those at $E=0.07$ J, and the lower values suggest higher wear resistance.
- It is known that as the radius of roundness R_s of the roughness peaks increases, the bearing surface of the roughness increases and the wear resistance of a certain surface increases. The KW and NW electrode coatings take the highest R_s values, followed by TiB_2-TiAl .
- For ESD, the maximum wave height W_t also increases compared to the original uncovered surface, which is unfavourable in the case of surface contact, since the effective contact areas decrease and the contact pressure increases.

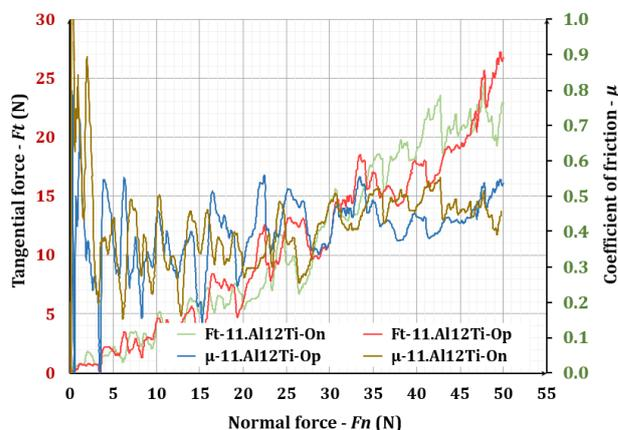
The summary of the results shows that the values of the coating roughness parameters are mainly determined by the pulse energy and the type of electrode material, and by the initial substrate roughness. As it has been found, after ESD on titanium surfaces with initial roughness $R_a \leq 3 \mu m$, most of the roughness parameters increase, i.e. the roughness of the coated surface worsens. Similar results to the present ones after nitrocarburization treatment are reported in [21].

3.2 Study of tribological characteristics of coatings

Fig. 7 shows the coefficients μ and friction force F_t of the AlSi12 electrode ESD coatings deposited at pulse energy $E=0.03$ J and 0.07 J as a function of the normal load F_n . It can be observed that at different normal loads the coefficient of friction of coatings deposited at $E=0.07$ J is about 10÷15% higher than that at $E=0.03$ J. The initial fluctuations of the friction coefficient at load F_n up to 15÷20 N are also higher.



(a) AlSi12 coatings, $E=0.03$ J

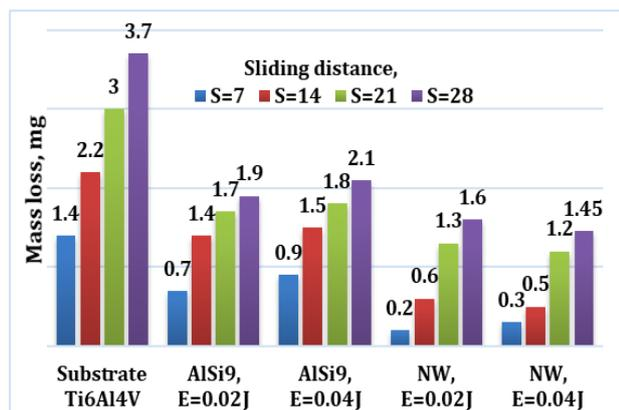


(b) AlSi12 coatings, $E=0.07$ J

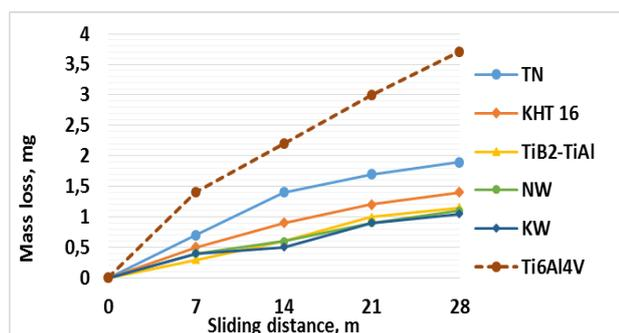
Fig. 7. The friction coefficient and friction force versus normal load for AlSi12 coatings deposited on Ti6Al4V with energy $E=0.03$ J and $E=0.07$ J.

Apparently, these differences are due to the higher values of the coating roughness parameters as a result of the higher pulse energy, as well as to the larger amount of wear resistant phases, higher thickness and microhardness of the coatings at $E=0.07$ J. Therefore, the differences in the coefficient of friction of the coatings obtained at the two pulse energies are relatively small, despite the significant differences in their roughness parameters. Similar results are obtained for the coatings of the other studied electrodes [26], where the values of the coefficient of friction of the coatings obtained with different pulse energies are in the range of $0.4 \div 0.5$. The obtained values are similar and even lower than those reported by [21,27], where the coefficient of friction of coated titanium surfaces is reported to be 0.57 [27].

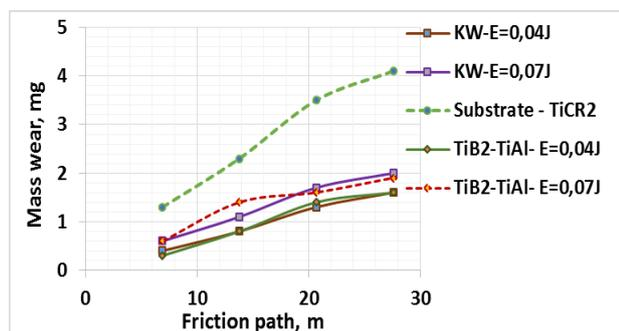
The wear of coatings deposited by LESD and ESD with the studied electrodes on Ti6Al4V is presented in Fig. 8.



(a) LESD with AlSi9 and NW electrodes



(b) ESD at pulse energy E=0.04 J

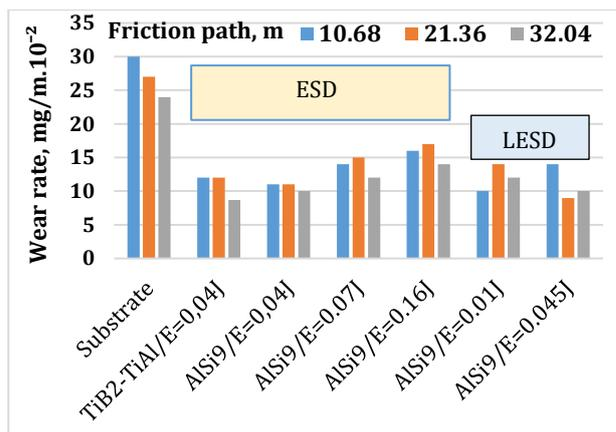


(c) ESD with KW and TiB₂-TiAl electrodes

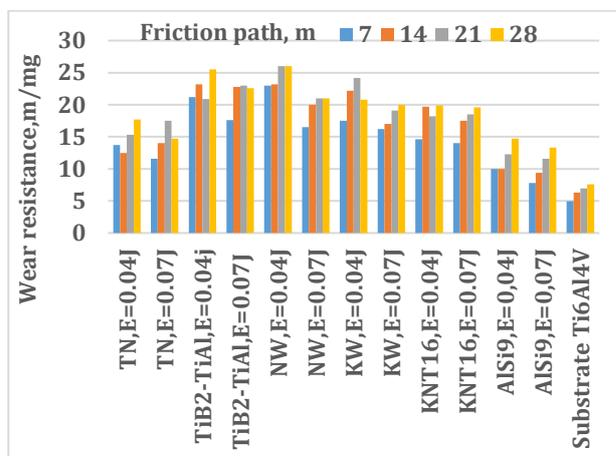
Fig. 8. Mass loss vs. sliding distance of tested coatings on Ti6Al4V alloy obtained by LESD and ESD processes at different pulse energies.

Fig. 9 shows the effect of pulse energy on the wear intensity and wear resistance of ESD and LESD coatings of the studied electrodes on technical titanium –Ti-GR2.

In contrast to mechanical processing, where only the influence of roughness parameters on wear can be distinguished and accounted for [17-21,28], in wear-resistant coatings and ESD there is a simultaneous complex influence of both roughness and changed composition, structure and properties of the coatings and differentiation of these two sides is complicated [10-13,15,22-24,26,27,29].



(a) ESD and LESD with TiB₂-TiAl and AlSi9 electrodes



(b) ESD at E=0.04 J and E=0.07 J

Fig. 9. Effect of pulse energy on wear intensity (a), and wear resistance (b) of ESD and LESD coatings on titanium Ti-GR2.

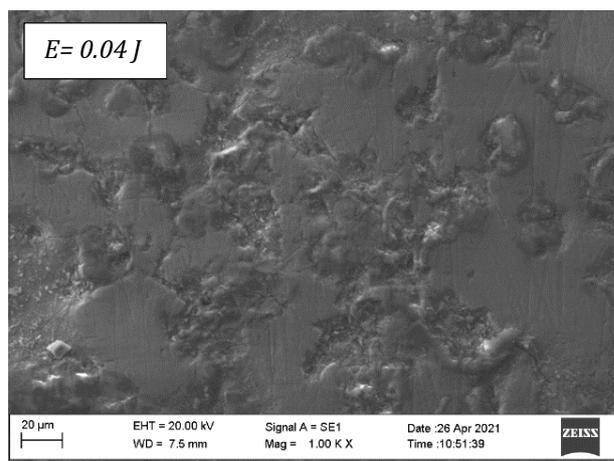
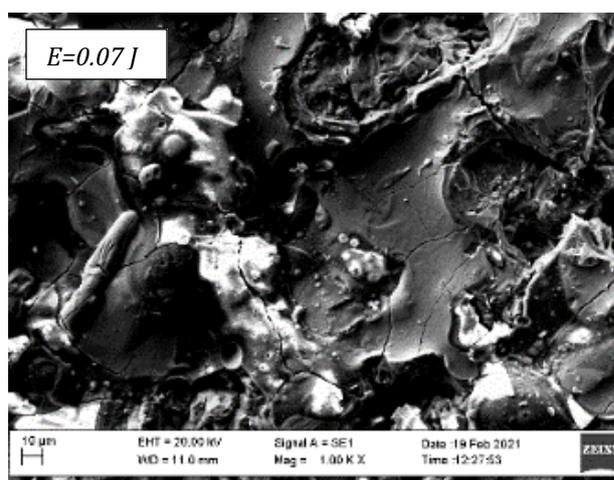
From the obtained results (Fig. 7, 8, and 9) and our previous studies [15,22-24,26] the following statements can be suggested:

- After ESD and LESD, wear and wear intensity decrease, respectively, the wear resistance of coated surfaces increases up to 3-4 times compared to that of uncoated surfaces (Fig. 9). Samples with coatings applied at energy $E=0.03\div 0.04$ J show the least wear. Apparently, at lower energies wear is mainly affected by the content of wear-resistant phases, higher microhardness and changes in the structure of the surface layer, and not so much by the roughness parameters. It is obvious that at pulse energy up to 0.04 J the negative influence of the roughness is compensated by the thickness, composition and structure of the coatings;
- With further increase in pulse energy above 0.04 J, the wear shows an increasing trend. At $E=0.16$ J the effect of ESD decreases and the

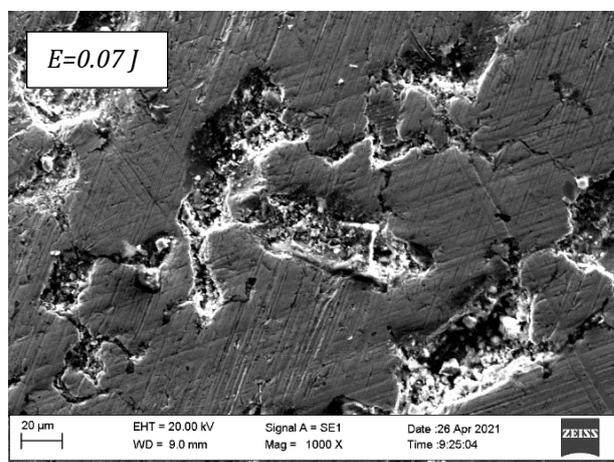
wear resistance assumes values up to $1.8 \div 2.2$ times higher than those of the uncoated substrate (Fig. 9a), or lower than those of surfaces coated with $E=0.03 \div 0.04$ J. It has been established that with increase in pulse energy above 0.04 J, all coating roughness parameters increase, like R_t , R_w , R_z , R_{max} , R_k+R_{pk} increase stronger. Therefore, the increase of those parameters starts to have a predominant influence on the wear and the higher amount of wear resistant phases in the coatings is unable to compensate the negative influence of those parameters, resulting in a decrease of the wear resistance. The specific values of the above parameters at $E=0.04$ J are different for different electrodes. Based on the results obtained in this work, for each of the electrodes used, can be determined with reasonable accuracy a limit values of R_t , R_w , R_z , R_{max} and R_k+R_{pk} , after exceeding of which, the wear begins to decrease. It has been observed that the influence of the universal parameter R_a on wear is to a lesser extent than that of R_t , R_w , R_z , R_{max} and the sum R_k+R_{pk} . Nevertheless, as the values of R_a are to some extent proportional to the values of the parameters above, it can be considered that for coatings with values of $R_a > \approx 3.5 \mu\text{m}$ the wear resistance shows a decreasing trend;

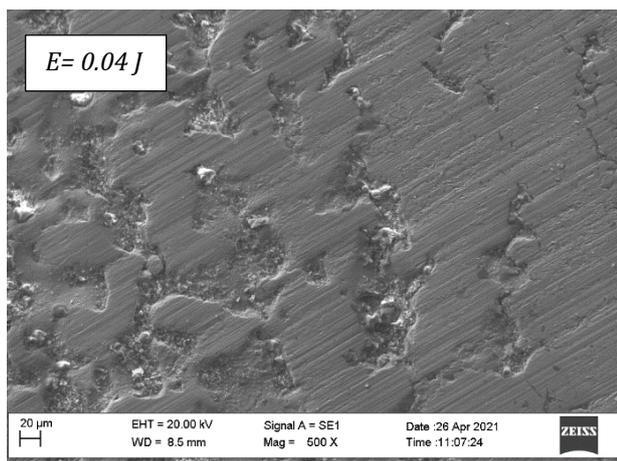
- The comparison of the wear resistance of the coated titanium substrates with the used electrodes shows that the coated specimens with electrode $\text{TiB}_2\text{-TiAl}$ nano, NW and KW have up to 20-35 % higher wear resistance than that of KNT16, TN and AlSi electrodes. This result is in agreement with the conclusions in references [6,13,26,30,31] where WC and NiCrBSi self-fluxing alloys have been used for wear resistant coatings;
- The analysis of the wear traces Fig. 10 shows that the wear mechanism of ESD coatings on titanium surfaces is similar. The predominant types of wear are abrasive and adhesive. The wear of the coated surfaces starts from the unmelted, transferred by brittle fracture electrode particles, which are not strongly bonded to the substrate, and from the highest peaks of the micro irregularities, which under the action of the abrasive particles and the friction force are broken down and detached from the coating. Clearly visible in Fig. 10a are traces of the breakdown and detachment

of the highest peaks and of the transported by brittle fracture particles at the beginning of friction. It can be observed that at $E=0.07$ J the fracture traces are larger and deeper than those of the coating at $E=0.04$ J. Due to the strong metallurgical bond, particles from the coating are detached together with particles from the surface of the substrate, forming craters on its surface.

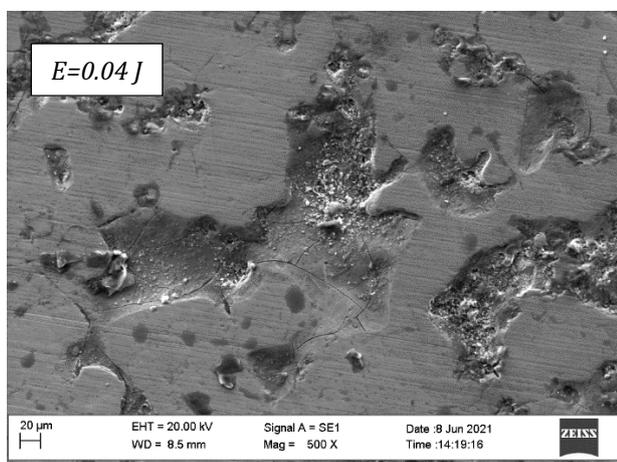
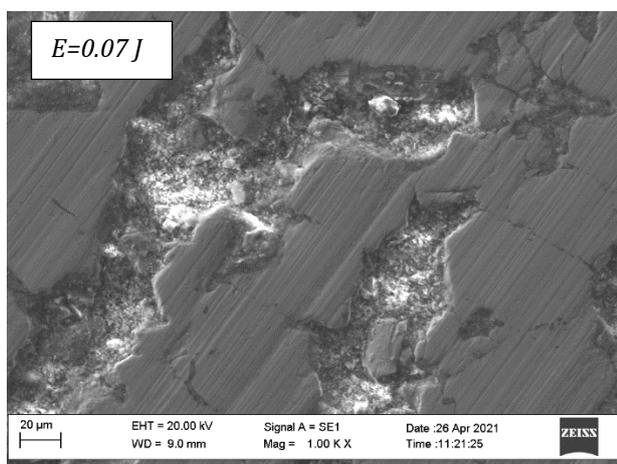


(a) Friction path 0.2 m





(b) Friction path 14 m



(c) Friction path 28 m

Fig. 10. SEM images of wear patterns

Because at $E > 0.04$ J the height of the irregularities and the peak sizes are bigger, the depth and size of the formed craters are also bigger - Fig. 10b. The detached solid particles get stuck between the friction surfaces accelerating the wear intensity. It can be observed from Fig. 10b and Fig. 10c that in surfaces formed with the smaller pulse energy $E = 0.04$ J the amount of formed craters is higher,

but their size and depth are much smaller than those formed at high energy. Clearly visible are the scratch traces caused by the abrasive particles of the grinding paper.

From the data obtained, it can be concluded that the wear of the produced coatings is due to the breakdown and shear of the high peaks and also to the scratching, caused by the abrasive particles. However, due to their higher hardness and good ductility, the coatings slow down the development of wear over time providing increased wear resistance to the coated surfaces. From the results obtained, it is found that no mathematically accurate correlation can be identified between wear and the roughness parameters studied. It is clear that the increased thickness will favourably affect the wear resistance, but the related occurrence of higher roughness, surface defects and the presence of particles carried by the electrode in an incompletely melted state, which are not well attached to the substrate, contribute to the increase of wear. When the pulse energy increases above certain values different for the different electrode-substrate pairs used, the negative influence of roughness becomes predominant and the effect of ESD begins to decrease. Therefore, in order to reduce wear and increase the effect of ESD, it is necessary to reduce the values of the most influencing roughness parameters, i.e. the height and size of the micro-roughness peaks, i.e. R_t , R_w , R_z , R_{max} and the sum $R_k + R_{pk}$.

3.3 Some guidelines for reducing the roughness of ESD coatings

The results of our present and previous studies [12,15,16,22-24,26] and the literature data [10,13,25,27,30,32] show that the following approaches are possible to obtain on titanium surfaces uniform ESD coatings with reduced roughness higher thickness:

- To reduce the energy of single pulses (current, capacitance and pulse duration) [10, 12,13,16,25,27,33-35]. This will result in coatings with fewer defects and lower roughness, but also lower thickness and the formation of a smaller amount of wear resistant phases and compounds in the coating composition. At the same time, however, the use of lower energy creates conditions for the

formation of a higher amount of amorphous and nanostructured phases in the composition of coatings, which, according to many authors [12,13,25,33-35], favourably affects their wear and corrosion resistance;

- The use of ESD and LESD with rotating electrode, low pulse duration - up to 30-40 μs and high pulse frequency above 1 kHz, is another possibility to simultaneously reduce the roughness and increase the thickness of coatings, combined with the formation of a larger amount of amorphous and nanostructured phases [12,14,22, 25, 34,35];
- Creation of coatings with 3 and 4 times consecutive electrode passes, the first passes with high pulse energy and the last with low pulse energy and specially selected electrodes - for example graphite [9,10,14,36], or low melting materials [13,23-25,33-35], as well as the AlSi alloys used in these studies, which "spill" onto the plated surface filling the pores and reducing the roughness. This method allows reducing the roughness of the coatings to $R_a \approx 2.5\text{-}3 \mu\text{m}$;
- If lower roughness is required, mechanical processing can be used - polishing, grinding, etc. However, these treatments remove the top layer of the coating, which contains the largest amount of wear-resistant, amorphous and nanostructured phases, which is unfavorable for wear resistance. The most effective additional treatments are mechanical or ultrasonic plastic deformation, or laser texturing [18]. However, the use of these treatments is time and cost consuming.

4. CONCLUSIONS

As the pulse energy changes, so do the topography, texture and roughness of the resulting coatings. Coatings with roughness $R_a=1.5\text{-}5 \mu\text{m}$, thickness $\delta=8\text{-}25 \mu\text{m}$, microhardness HV up to 14 GPa and up to 2-3 times higher wear resistance than that of titanium alloy were obtained at different pulse energy. The presented results of the studies of the variation of the height, step and functional parameters of the roughness of the coatings as a function of the energy and pulse parameters and the type of electrode material allow a preliminary tentative assessment of the tribological properties of the coatings.

The obtained results show the relationship between the technological parameters of the mode and pulse energy for ESD and the quality parameters of the coated surface and enable the obtaining surface layers with previously known roughness, thickness and microhardness parameters.

The lowest roughness, but also the lowest thickness under the same energy conditions was obtained using KNT16, TiN, AlSi, TiB₂-TiAl electrodes, and the highest - with tungsten containing "NW" and "KW" electrodes.

At an initial roughness of titanium substrates $R_a \geq 4 \mu\text{m}$, the use of ESD with low-energy pulses $E \leq 0.04 \text{ J}$, enables its reduction and removal the surface defects by obtaining uniform and smooth coatings.

At an initial substrate roughness $R_a < 3 \mu\text{m}$, ESD processing increases the initial roughness parameters. The R_{sk} and R_{ku} parameters appear unrelated to the pulse energy.

As the pulse energy increases to $0.03 \div 0.045 \text{ J}$, the wear resistance of the coated surfaces increases in parallel with the roughness. At $E \geq 0.05 \text{ J}$, the effect of ESD on wear resistance shows a gradual decreasing trend due to the increasing unfavorable effect of increasing roughness.

The roughness parameters that most influence the wear resistance of the ESD surfaces are R_t , R_w , R_z , R_{max} and the sum $R_k + R_{pk}$.

Acknowledgement

The present work is based on researches that are funded from the Bulgarian National Science Fund of the Ministry of Education and Science under the project №KP-06-H37/19 "Technological features and regularities of creation of new high wear resistant composite coatings on titanium alloys by electrical spark deposition process" and project BG05M2OP001-1.001-0008.

This paper has been presented at the 18th International Conference on Tribology – SERBIANTRIB '23 17-19 May 2023, Kraguevac, Serbia.

REFERENCES

- [1] H. Garbacz, P. Wieceński, M. Ossowski, M. G. Ortore, T. Wierzchoń, and K. J. Kurzydłowski, "Surface engineering techniques used for improving the mechanical and tribological properties of the Ti6Al4V alloy," *Surface & Coatings Technology*, vol. 202, no. 11, pp. 2453–2457, Feb. 2008, doi: [10.1016/j.surfcoat.2007.08.068](https://doi.org/10.1016/j.surfcoat.2007.08.068).
- [2] F. Yildiz, A. F. Yetim, A. Alsaran, and A. Çelik, "Plasma nitriding behavior of Ti6Al4V orthopedic alloy," *Surface & Coatings Technology*, vol. 202, no. 11, pp. 2471–2476, Feb. 2008, doi: [10.1016/j.surfcoat.2007.08.004](https://doi.org/10.1016/j.surfcoat.2007.08.004).
- [3] C. Martini and L. Ceschini, "A comparative study of the tribological behaviour of PVD coatings on the Ti-6Al-4V alloy," *Tribology International*, vol. 44, no. 3, pp. 297–308, Mar. 2011, doi: [10.1016/j.triboint.2010.10.031](https://doi.org/10.1016/j.triboint.2010.10.031).
- [4] M. Walczak, K. Pasierbiewicz, and M. Szala, "Effect of Ti6Al4V substrate manufacturing technology on the properties of PVD nitride coatings," *Acta Physica Polonica A*, vol. 142, no. 6, pp. 723–732, Dec. 2022, doi: [10.12693/aphyspola.142.723](https://doi.org/10.12693/aphyspola.142.723).
- [5] A. Anand, M. Das, B. Kundu, V. K. Balla, S. Bodhak, and S. Gangadharan, "Plasma-Sprayed Ti6Al4V Alloy Composite Coatings Reinforced with In Situ Formed TiB-TiN," *Journal of Thermal Spray Technology*, vol. 26, no. 8, pp. 2013–2019, Nov. 2017, doi: [10.1007/s11666-017-0651-5](https://doi.org/10.1007/s11666-017-0651-5).
- [6] E. Zdravecká, M. Ondáč, and J. Tkáčová, "Tribological Behavior of Thermally Sprayed Coatings with Different Chemical Composition and Modified by Remelting," *Tribology in Industry*, vol. 41, no. 4, pp. 463–470, Dec. 2019, doi: [10.24874/ti.2019.41.04.01](https://doi.org/10.24874/ti.2019.41.04.01).
- [7] G. Dezső, F. Szigeti, and G. Varga, "Surface hardness modification of selective laser melted Ti6Al4V parts by sliding friction diamond burnishing," *Periodica Polytechnica Mechanical Engineering*, vol. 67, no. 1, pp. 59–69, Jan. 2023, doi: [10.3311/ppme.21124](https://doi.org/10.3311/ppme.21124).
- [8] L. C. Zhang, L. Chen, and L. Wang, "Surface modification of titanium and titanium alloys: technologies, developments, and future interests," *Advanced Engineering Materials*, vol. 22, pp. 1–37, no. 5, May 2020, doi: [10.1002/adem.202070017](https://doi.org/10.1002/adem.202070017).
- [9] V.V. Mikhailov, A.E. Gitlevich, A.D. Verkhoturov, A.I. Mikhaylyuk, A.V. Belyakovsky, L.A. Konevtsov, "Electrospark alloying of titanium and its alloys, physical and technological aspects and the possibility of practical use," *Surface engineering and applied electrochemistry*, vol. 49, no. 5, pp. 21–44, 2013.
- [10] Z. Zhengchuan, L. Guanjun, I. Konoplianchenko, V. B. Tarelnyk, "A review of the electro-spark deposition technology," *Bulletin of Sumy National Agrarian University, Mechanization and Automation of Production Processes*, vol. 44, no. 2, pp. 45–53, May 2022, doi: [10.32845/msnau.2021.2.10](https://doi.org/10.32845/msnau.2021.2.10).
- [11] J.L. Reynold, R.L. Holdren, L.E. Brown, "Electro-Spark Deposition," *Advanced Materials & Processes*, vol. 161, no. 3, pp. 35–37, Mar. 2003.
- [12] T. Penyashki et al., "Improving Surface Properties of Titanium Alloys by Electrospark Deposition with Low Pulse Energy," *Surface Engineering and Applied Electrochemistry*, vol. 58, no. 6, pp. 580–593, Dec. 2022, doi: [10.3103/s1068375522060126](https://doi.org/10.3103/s1068375522060126).
- [13] E. A. Levashov, A. E. Kudryashov, Yu. S. Pogozev, P. V. Vakaev, E. I. Zamulaeva, and T. A. Sviridova, "Specific features of formation of nanostructured electrospark protective coatings on the OT4-1 titanium alloy with the use of electrode materials of the TiC-Ti₃AlC₂ system disperse-strengthened by nanoparticles," *Russian Journal of Non-Ferrous Metals*, vol. 48, no. 5, pp. 362–372, Oct. 2007, doi: [10.3103/s1067821207050100](https://doi.org/10.3103/s1067821207050100).
- [14] V.V. Mikhailov, E.A. Pasinkovsky, K.A. Bachu, P.V. Peretyatku, "On the issue of electrospark alloying of titanium and its alloys," *Surface engineering and applied electrochemistry*, vol. 42, no. 3, pp. 106–111, 2006.
- [15] M. K. Kandeve et al., "Abrasive wear resistance of electrospark coatings on titanium alloys," *Tribology in Industry*, vol. 44, no. 1, pp. 132–142, Mar. 2022, doi: [10.24874/ti.1143.06.21.09](https://doi.org/10.24874/ti.1143.06.21.09).
- [16] G. Kostadinov et al., "Surface topography and roughness parameters of electrospark coatings on titanium and nickel alloys," *Applied Engineering Letters*, vol. 6, no. 3, pp. 89–98, Jan. 2021, doi: [10.18485/aeletters.2021.6.3.1](https://doi.org/10.18485/aeletters.2021.6.3.1).
- [17] P. L. Menezes and S. V. Kailas, "Influence of roughness parameters of harder surface on coefficient of friction and transfer layer formation," *International Journal of Surface Science and Engineering*, vol. 2, no. 1/2, p. 98, Jan. 2008, doi: [10.1504/ijsurfse.2008.018971](https://doi.org/10.1504/ijsurfse.2008.018971).
- [18] A. Vencl, L. Ivanović, B. Stojanović, E. Zadorozhnaya, S. Miladinović, and P. Svoboda, "Surface texturing for tribological applications: a review," *Proceedings on Engineering Sciences*, vol. 1, no. 1, pp. 227–239, May 2019, doi: [10.24874/pes01.01.029](https://doi.org/10.24874/pes01.01.029).
- [19] F. Svahn, Å. Kassman-Rudolph, and E. Wallén, "The influence of surface roughness on friction and wear of machine element coatings," *Wear*, vol. 254, no. 11, pp. 1092–1098, Oct. 2003, doi: [10.1016/s0043-1648\(03\)00341-7](https://doi.org/10.1016/s0043-1648(03)00341-7).

- [20] B. Nedić, L. Slavković, S. Đurić, D. Adamović, and S. Mitrović, "Surface roughness quality, friction and wear of parts obtained on 3D printer," *Proceedings on Engineering Sciences*, vol. 1, no. 1, pp. 98–103, May 2019, doi: [10.24874/pes01.01.013](https://doi.org/10.24874/pes01.01.013).
- [21] E. Ghelloudj, M. T. Hannachi, and H. Djebaili, "Experimental investigation on roughness parameters of 42CrMo4 steel surface during nitrocarburizing treatment," *Tribology in Industry*, vol. 44, no. 4, pp. 599–607, Dec. 2022, doi: [10.24874/ti.1304.05.22.10](https://doi.org/10.24874/ti.1304.05.22.10).
- [22] G. Kostadinov, T. Penyashki, A. Nikolov, R. Dimitrova et al., "Geometric characteristics, composition and structure of coatings of WC-TiB₂-B₄C- Ni-Cr-B-Si-C electrodes formed on 3D printing titanium and steels by contactless electrospark deposition," *Materials, Methods & Technologies*, vol. 16, pp. 160-171, Nov. 2022.
- [23] G. Kostadinov, T. Penyashki, M. Petrzhik, E. Kostitcyna et al., "Obliteration of surface defects in 3D printing of metals by reactive electro spark surface modification," *J. Industry 4.0*, no. 4, pp. 126-130, Jun. 2022.
- [24] G. Kostadinov, T. Penyashki, V. Kamburov et al., "Possibilities for improving the surface quality of structural steels, invar and titanium alloys through reactive electrospark treatment with electrodes of an aluminum-silicon alloys," *Journal of International Scientific Researches Materials, Methods & Technologies*, vol. 15, pp. 105-122, Oct. 2021.
- [25] S. K. Mukanov, A. E. Kudryashov, M. I. Petrzhik, "Surface modification of titanium VT6 alloy obtained by additive technologies using reactive electrospark treatment," *Physics and chemistry of material processing*, no. 3, pp. 30-39, 2021.
- [26] T. Penyashki, G. Kostadinov, M. K. Kandeve, V. Kamburov, A. Nikolov, and R. Dimitrova, "Abrasive and Erosive Wear of Ti6Al4V Alloy with Electrospark Deposited Coatings of Multicomponent Hard Alloys Materials Based of WC and TiB₂," *Coatings*, vol. 13, no. 1, p. 215, Jan. 2023, doi: [10.3390/coatings13010215](https://doi.org/10.3390/coatings13010215).
- [27] W. Wang and C. Han, "Microstructure and wear resistance of Ti6Al4V coating fabricated by Electro-Spark Deposition," *Metals*, vol. 9, no. 1, p. 23, Dec. 2018, doi: [10.3390/met9010023](https://doi.org/10.3390/met9010023).
- [28] S. Đurovic et al., "Modeling and Prediction of Surface Roughness in the End Milling Process using Multiple Regression Analysis and Artificial Neural Network," *Tribology in Industry*, vol. 44, no. 3, pp. 540–549, Sep. 2022, doi: [10.24874/ti.1368.07.22.09](https://doi.org/10.24874/ti.1368.07.22.09).
- [29] F. O. Kolawole, S. K. Kolawole, L. B. Varela, A. Kraszczuk, M. A. Ramírez, and A. P. Tschiptschin, "Effect of substrate surface roughness on the tribological properties of DLC-H coatings on Tappet valve," *Tribology in Industry*, vol. 43, no. 2, pp. 189–199, Jun. 2021, doi: [10.24874/ti.927.07.20.11](https://doi.org/10.24874/ti.927.07.20.11).
- [30] V. D. Kalyankar and S. P. Wanare, "Comparative investigations on microstructure and slurry abrasive wear resistance of NiCrBSi and NiCrBSi-WC composite hardfacings deposited on 304 stainless steel," *Tribology in Industry*, vol. 44, no. 1, pp. 199–211, Jun. 2022, doi: [10.24874/ti.1075.03.21.05](https://doi.org/10.24874/ti.1075.03.21.05).
- [31] A. Vencl, M. Mrdak, and P. Hvizdoš, "Tribological Properties of WC-Co/NiCrBSi and Mo/NiCrBSi Plasma Spray Coatings under Boundary Lubrication Conditions," *Tribology in Industry*, vol. 39, no. 2, pp. 183–191, Jun. 2017, doi: [10.24874/ti.2017.39.02.04](https://doi.org/10.24874/ti.2017.39.02.04).
- [32] J. Tang, "Mechanical and tribological properties of the TiC-TiB₂ composite coating deposited on 40Cr-steel by electro spark deposition," *Applied Surface Science*, vol. 365, no. 1, pp. 202–208, Mar. 2016, doi: [10.1016/j.apsusc.2015.12.198](https://doi.org/10.1016/j.apsusc.2015.12.198).
- [33] J. Milligan, D. W. Heard, and M. Brochu, "Formation of nanostructured weldments in the Al-Si system using electrospark welding," *Applied Surface Science*, vol. 256, no. 12, pp. 4009–4016, Apr. 2010, doi: [10.1016/j.apsusc.2010.01.068](https://doi.org/10.1016/j.apsusc.2010.01.068).
- [34] S. Cadney, G. R. Goodall, G. Kim, A. L. Morán, and M. Brochu, "The transformation of an Al-based crystalline electrode material to an amorphous deposit via the electrospark welding process," *Journal of Alloys and Compounds*, vol. 476, no. 1–2, pp. 147–151, May 2009, doi: [10.1016/j.jallcom.2008.09.017](https://doi.org/10.1016/j.jallcom.2008.09.017).
- [35] E.I. Zamulaeva, E.A. Levashov, A.E. Kudryashov, P.V. Vakaev, M.I. Petrzhik, "Electrospark coatings deposited onto an Armco iron substrate with nano- and microstructured WC-Co electrodes: Deposition process, structure, and properties," *Surface & Coatings Technology*, vol. 202, no. 15, pp. 3715–3722, Apr. 2008, doi: [10.1016/j.surfcoat.2008.01.008](https://doi.org/10.1016/j.surfcoat.2008.01.008).
- [36] V. Tarelnyk et al., "ElectroSpark Graphite Alloying of Steel Surfaces: Technology, Properties, and Application," *Surface Engineering and Applied Electrochemistry*, vol. 54, no. 2, pp. 147-156, Mar. 2018, doi: [10.3103/s106837551802014x](https://doi.org/10.3103/s106837551802014x).